

COIN CDN 2012-1-57 - CU ALLOY - LATE ROMAN TIMES - SWITZERLAND

Artefact name Coin CdN 2012-1-57

Authors Rey-Bellet, Bernadette (, None) & Naima. Gutknecht (HE-Arc CR, Neuchâtel, Neuchâtel, Switzerland) & Valentina. Valbi (Laboratoire Métallurgie et Culture LMC-IRAMAT-CNRS-UTBM, Belfort, Franche-Comté, France)

Url /artefacts/1369/

∨ The object



Fig. 1: Views of both sides of a coin from the "Peney hoard" with blue/green and white corrosion products,

Credit MAHG, B. Rey-Bellet.

∨ Description and visual observation

Description of the artefact	Coin with blue/green and localised white corrosion products. The coin is probably an imitation. Diameter: about 1.2cm.
Type of artefact	coin
Origin	Peney, Genève, Geneva, Switzerland
Recovering date	1960
Chronology category	Late roman times
chronology tpq	<input type="text" value="388"/> A.D. ▼
chronology taq	<input type="text" value=""/> ---- ▼
Chronology comment	
Burial conditions / environment	Soil
Artefact location	Musée d'art et d'histoire, Genève, Geneva
Owner	Musée d'art et d'histoire, Genève, Geneva
Inv. number	CdN 2012-1-57
Recorded conservation data	No conservation treatment reported

Complementary information

Object recovered in 1960 at Peney, Geneva, Switzerland in a hoard containing 4000 coins. Around 1400 coins from the hoard are conserved at the Art and History Museum of Geneva.

Study area(s)

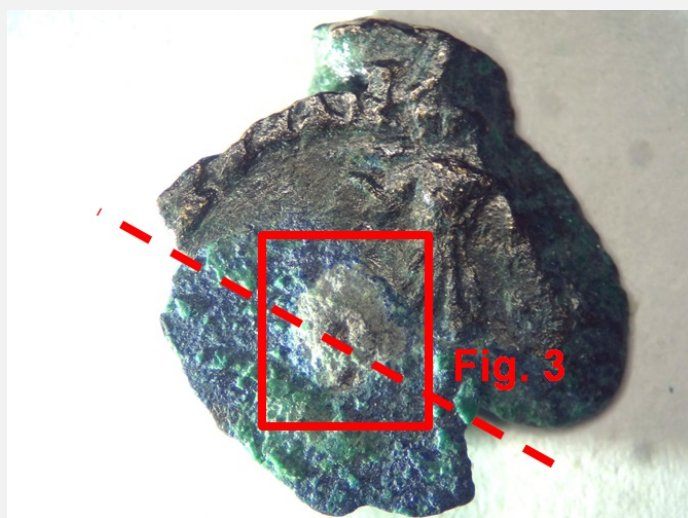


Fig. 2: Location of the detail (Fig. 3) and of the sampling for cross-section,

Credit MAHG, B.Rey-Bellet/ HE-Arc CR, N.Gutknecht.

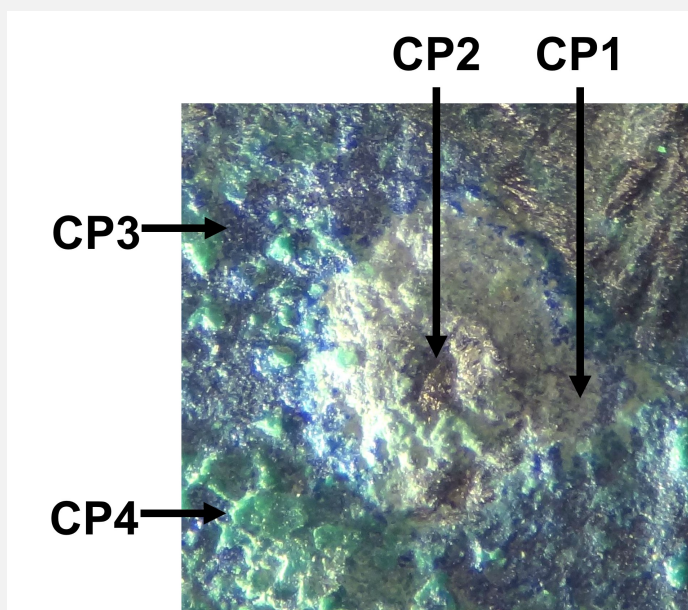


Fig. 3: Detail of the corrosion structure with reference to Fig. 4,

Credit MAHG, B.Rey-Bellet/ HE-Arc CR, N.Gutknecht.

Binocular observation and representation of the corrosion structure

The schematic representation below gives an overview of the corrosion structure encountered on the coin from a first visual macroscopic observation.

Stratum	Type of stratum	Principal characteristics
CP1	Corrosion product	Cluster, light yellow, thin, scattered, compact, powdery, very soft
CP2	Corrosion product	Lens-shaped, light brown, thick, isolated, non-compact, powdery, soft
CP3	Corrosion product	Cluster, blue, medium, scattered, compact, brittle, soft
CP4	Corrosion product	Cluster, dark green, medium, scattered, compact, severable, soft
M1	Metal	Light grey, metallic, continuous, compact, tough, soft

Table 1: Description of the principal characteristics of the strata as observed under binocular microscope according to Bertholon's

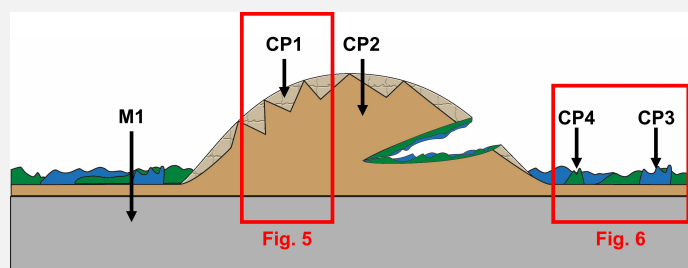


Fig. 4: Stratigraphic representation of the corrosion structure of the coin by macroscopic and binocular observation with indication of the corrosion structures used to build the MiCorr stratigraphies of Figs. 5 and 6 (red squares),

Credit HE-Arc CR, N.Gutknecht.

✎ MiCorr stratigraphy(ies) – Bi

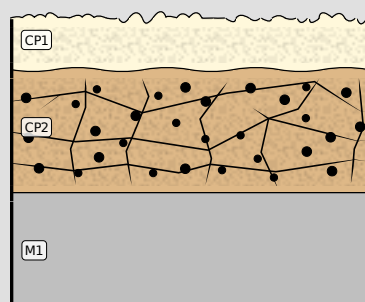


Fig. 5: Stratigraphic representation of the corrosion structure of the coin observed macroscopically under binocular microscope using the MiCorr application. The characteristics of the strata are only accessible by clicking on the drawing that redirects you to the search tool by stratigraphy representation, Credit MAHG, B.Rey-Bellet/HE-Arc CR, N.Gutknecht.

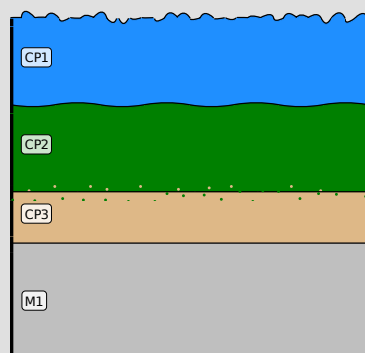
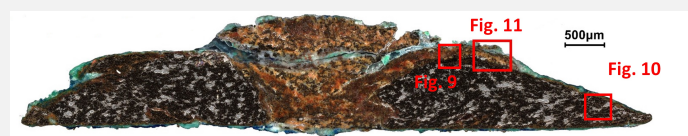


Fig. 6: Stratigraphic representation of the corrosion structure of the coin observed macroscopically under binocular microscope using the MiCorr application. CP1 is CP3 and CP2 is CP4 in Fig. 4. The characteristics of the strata are only accessible by clicking on the drawing that redirects you to the search tool by stratigraphy representation, Credit MAHG, B.Rey-Bellet/HE-Arc CR, N.Gutknecht.

✎ Sample(s)



Credit LMC-CNRS, V. Valbi.

Fig. 7: Micrograph of the cross-section of the sample taken from the coin (Fig. 2) in dark field showing the location of Figs. 9 to 11,

Description of sample

The cross-section corresponds to a cut of the coin in half (Fig. 2) and is representative of the entire thickness of the coin's body. A metallic core is present below the corrosion layers (Fig. 7).

Alloy

Cu alloy

Technology

Cast and cold worked (with final annealing?)

Lab number of sample

BC57

Sample location

Musée d'art et d'histoire, Genève, Geneva

Responsible institution Musée d'art et d'histoire, Genève, Geneva

Date and aim of sampling June 2021

Complementary information

None.

Analyses and results

Analyses performed:

Non-invasive approach

- XRF with handheld portable X-ray fluorescence spectrometer (NITON XL3t 950 Air GOLDD+, Thermo Fischer®). General Metal mode, acquisition time 60s (filters: Li20/Lo20/M20).

Invasive approach (on the sample)

- Optical microscopy: the sample is polished, then it is observed on a numerical microscope KEYENCE VHX-7000 in bright and dark field.

- Metallography: the polished sample is etched with alcoholic ferric chloride and observed by optical microscopy in bright field.

- SEM-EDS: the sample is coated with a carbon layer and analyses are performed on a SEM-FEG JEOL 7001-F equipped with a silicon-drift EDS Oxford detector (Aztec analysis software) with an accelerating voltage of 20 kV and probe current at about 9 nA. The relative error is considered of about 10% for content range <1mass%, and of 2% for content range of >1mass%.

- μ -Raman spectroscopy: it is performed on a HORIBA Labram Xplora spectrometer equipped with a 532 nm laser with 1800 grating, the laser power employed is between 0.04 and 0.55 mW with acquisition time varying between 1 and 5 minutes.

Non invasive analysis

The XRF analysis of coin CdN 2012-1-57 was carried out before sampling. All strata, from soil and corrosion products to metal, are analyzed at the same time. The metal is presumably a copper-lead-tin alloy, while the other elements detected (Fe, Si, Al) are from the environment.

Elements	mass %
Cu	46
Pb	46
Sn	3
Si	3
Fe	<1
Al	3

Table 2: Chemical composition of the surface of coin CdN 2012-1-57. Method of analysis: XRF, General Metal mode, acquisition time 60s (filters: Li20/LO20/M20). The results are rounded up to the nearest whole number, UR-Arc CR.

Metal

The central area of the sample is totally corroded.

EDX analysis (Table 3) of the residual metal on cross-section indicates that it is a Cu-Pb-Sn ternary alloy with a high percentage of Pb (25 wt%). This confirms XRF analysis (Table 2).

Elements	wt%
Cu	69
Pb	26
Sn	5

Table 3: Chemical composition (wt%) of the alloy over a general area of analysis, LMC-IRAMAT-CNRS-UTBM.

The sample presents on its whole thickness big Pb inclusions (50-200 μm , Figs. 8) homogeneously distributed. The metal has a heterogeneous microstructure. The microstructure is mostly dendritic with slip lines (Figs. 9-10) lines revealing that the object underwent cold working (Fig.9). Some areas show the presence of grain boundaries of polygonal grains (Fig.10) with slip lines, showing that the object also underwent local annealing, followed by cold working.



Fig. 8: Micrograph (similar to Fig. 7) of the cross-section of the sample taken from the coin (Fig.2) in bright field after chemical etching,

Credit LMC-CNRS, V. Valbi.

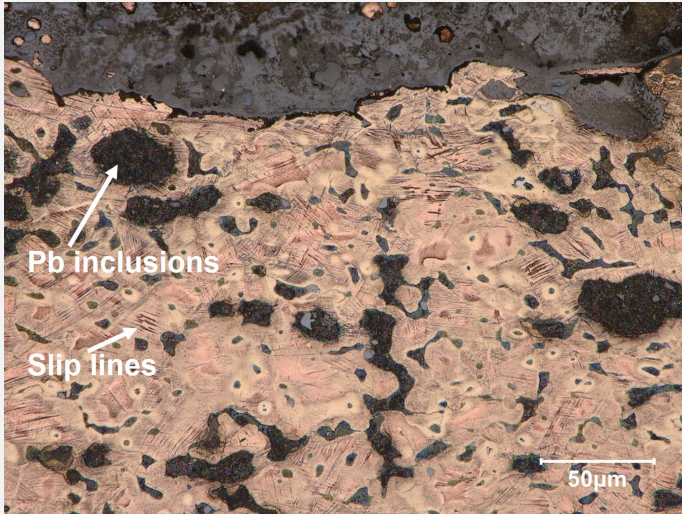


Fig. 9: Micrograph of the metal sample from Fig. 7 (detail), etched, bright field. Dendritic structure with slip lines are observed, as well as grey lead inclusions,

Credit LMC-CNRS, V. Valbi.

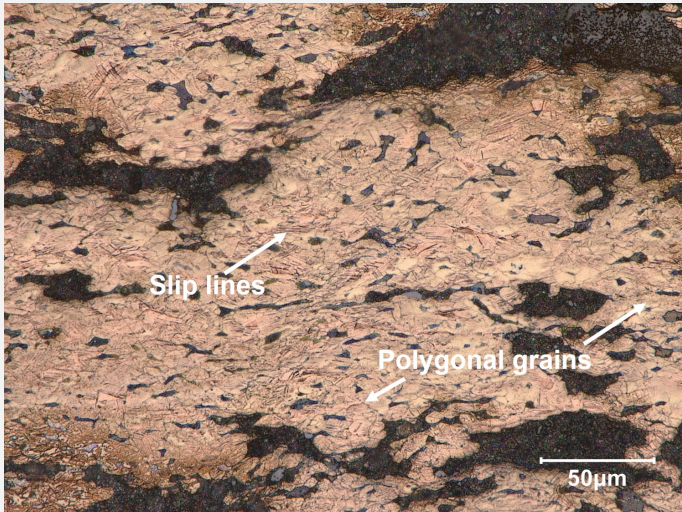


Fig. 10: Micrograph of the metal sample from Fig. 7 (detail), etched, bright field. with polygonal microstructure and slip lines,

Credit LMC-CNRS, V. Valbi.

Microstructure	Dendritic structure & limited grain structure (with twin lines)
First metal element	Cu
Other metal elements	Sn, Pb

Complementary information

None.

The observation of the sample in dark field mode (Fig.11) revealed the presence of an external discontinuous blue CP1 layer, a white/greenish CP2 layer and a thick internal orange CP3 layer.

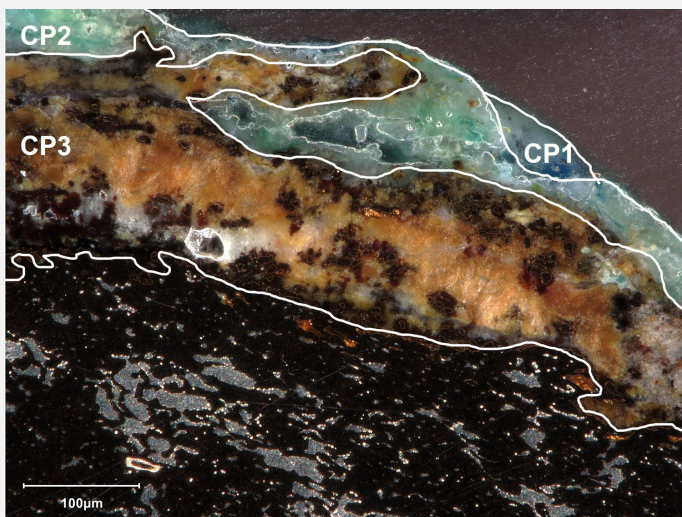
The EDX elemental analysis (Table 4, Fig.12) of the visually identified CPs by cross-sectional observation shows that the external CP1 is a Cu-based compound, while the white CP2 and the orange CP3 are lead-based corrosion products. Local Cl enrichments (3 wt%) and Cu uncorroded areas are observed in CP3.

μ -Raman analyses were performed on the identified strata (Fig.13). The Raman spectrum obtained on the blue CP1 layer corresponds to the one of azurite ($\text{Cu}_3(\text{CO}_3)_2(\text{OH})_2$). The Raman spectrum obtained on the white CP2 corresponds to cerussite (PbCO_3), while the orange CP3 layer corresponds to litharge (PbO).

The central area of the sample, which is totally corroded, shows the same stratigraphy described here and is mainly composed of litharge with small areas of uncorroded copper (CP3).

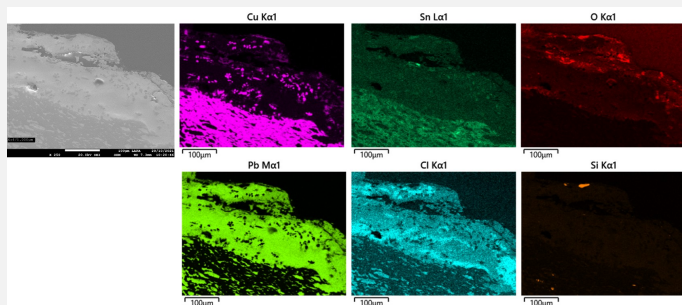
Elements	CP2	CP3
O	20	7
Cu	3	1
Pb	77	92

Table 4: Chemical composition (wt %) of the corrosion layers over a general area of analysis in cross-section, LMC-IRAMAT-CNRS-UTBM. Carbon is not quantified by SEM-EDX because the sample was carbon-coated.



Credit LMC-CNRS, V. Valbi.

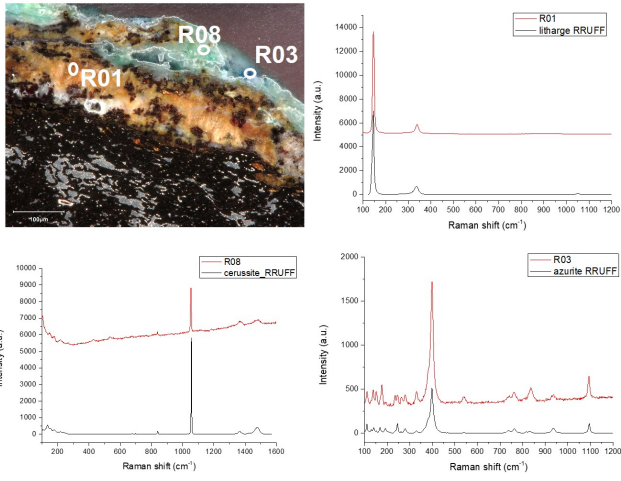
Fig. 11: Micrograph of the sample from Fig. 7 (detail), unetched, dark field with location of CP strata,



Credit LMC-CNRS, V. Valbi.

Fig. 12: SEM image, SE-mode, and elemental chemical distribution of Fig. 11,

Fig. 13: Raman points of analysis and corresponding spectra overlapped with reference spectra of litharge (RRUFFID=R060959), cerussite (RRUFFID=R060017) and azurite (RRUFFID=R050497),



Credit LMC-CNRS, V. Valbi.

Corrosion form Uniform

Corrosion type None

Complementary information

None.

✧ MiCorr stratigraphy(ies) – CS

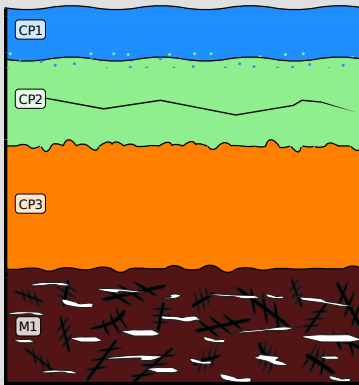
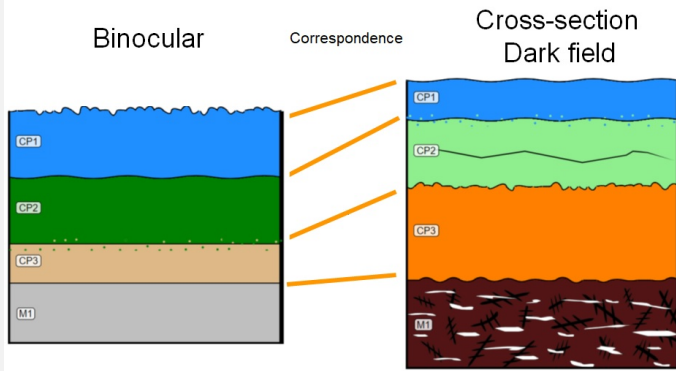


Fig. 14: Stratigraphic representation of the sample of the coin BL55 under dark field using the MiCorr application. The characteristics of the strata are only accessible by clicking on the drawing that redirects you to the search tool by stratigraphy representation. This representation was built according to Fig. 11, Credit LMC-CNRS, V.Valbi.

✧ Synthesis of the binocular / cross-section examination of the corrosion structure

The stratigraphies obtained by binocular and cross-section observation show a good matching (Fig. 15). The blue CP1 observed by binocular corresponds to the blue azurite CP1 observed by CS. The green CP2 observed by binocular is also present in the CS stratigraphy. The light brown CP3 observed by binocular corresponds to the orange CP3 in CS. In CS it was possible to differentiate the carbonate cerussite and the oxide litharge.

Fig. 15: Stratigraphic representation side by side of binocular view and cross-section (dark field),



Credit LMC-CNRS, V.Valbi/HE-Arc CR, N.Gutknecht.

Conclusion

The coin is composed of a Cu-Pb-Sn ternary bronze alloy with high Pb percentages (26 wt%). Pb is not soluble in the bronze metallic structure and high lead inclusions are observed throughout the whole metallic sample. The metallic microstructure reveals that the object has been cast and underwent cold working after local annealing (not well completed).

The external thin discontinuous corrosion products are composed of Cu-based hydroxycarbonate (azurite and probably malachite) formed by redeposition of copper with the carbonate ions from the burial environment. Lead corrosion products (litharge and cerussite) are observed as internal CPs. The presence of uncorroded Cu in the litharge layer shows that Pb is preferentially attacked. The central area of the sample, which is totally corroded, is also made of litharge with local areas of uncorroded copper. This shows that the central area of the sample had a similar composition as the rest of the sample (Cu-Pb-Sn ternary bronze). However, lead corrosion was accentuated in the central area so it is possible that this central area had a different Cu/Pb ratio from the beginning, but it is impossible to say if it was intentional or not.

This coin is part of a corpus of coins found in the same site and called "Peney Treasury". Two more coins were studied and have a MiCorr artefact sheet.

References

References on object and sample

1. MiCorr_Coin (white corrosion) CdN 2012-1-50
2. MiCorr_Coin (blue corrosion) CdN 2012-1-55

References on analytical methods and interpretation

3. Lafuente, B., Downs, R. T., Yang, H., Stone, N. (2015) The power of databases: the RRUFF project. In: Highlights in Mineralogical Crystallography, T. Armbruster and R. M. Danisi, eds. Berlin, Germany, W. De Gruyter, 1-30.
4. Scott, D. (2006) Metallography and microstructure of ancient and historic metals. J Paul Getty Museum Publications.
5. Švadlena J., Prošek T., Strachotová KC., Kouřil M. (2020). Chemical Removal of Lead Corrosion Products. Materials, 12 (24), 5672.
6. Quaranta M., Catelli E., Prati S., Scitutto G., Mazzeo R. (2014) Chinese archaeological artefacts: Microstructure and corrosion behaviour of high-lead bronzes. Journal of Cultural Heritage, 15 (3), 283-291.